THE JOURNAL OF BIOLOGICAL CHEMISTRY VOL. 286, NO. 45, pp. 39130–39140, November 11, 2011

Inner Mitochondrial Translocase Tim50 Interacts with 3β-Hydroxysteroid Dehydrogenase Type 2 to Regulate Adrenal and Gonadal Steroidogenesis*[S]

Received for publication, August 8, 2011, and in revised form, September 8, 2011 Published, JBC Papers in Press, September 19, 2011, DOI 10.1074/jbc.M111.290031

Kevin J. Pawlak[‡1], **Manoj Prasad**[‡1], **James L. Thomas**[§], **Randy M. Whittal**[¶], **and Himangshu S. Bose**[‡‖2]

From the [‡]*Mercer University School of Medicine and the* [‖]*Memorial University Medical Center, Savannah, Georgia 31404, the* [§]*Department of Biochemistry, Division of Basic Medical Sciences, Mercer University School of Medicine, Macon, Georgia 31207, and the* [¶]*Department of Chemistry, University of Alberta, Edmonton, Alberta T6G 2G2, Canada*

Background: The role of mitochondrial translocases in steroid hormone synthesis is investigated.
Results: Expression of inner mitochondrial translocase Tim50 is essential for DHEA and androstenedione synthesis.
Conclusion: Tim50 interacts with 3βHSD2 for steroid hormone synthesis.
Significance: During steroidogenesis, the flexibility of 3βHSD2 is essential to coordinate interaction between Tim50 and Tom22.

In the adrenals, testes, and ovaries, 3β-hydroxysteroid dehydrogenase type 2 (3βHSD2) catalyzes the conversion of pregnenolone to progesterone and dehydroepiandrostenedione to androstenedione. Alterations in this pathway can have deleterious effects, including sexual development impairment, spontaneous abortion, and breast cancer. 3βHSD2, synthesized in the cytosol, is imported into the inner mitochondrial membrane (IMM) by translocases. Steroidogenesis requires that 3βHSD2 acts as both a dehydrogenase and isomerase. To achieve this dual functionality, 3βHSD2 must undergo a conformational change; however, what triggers that change remains unknown. We propose that 3βHSD2 associates with IMM or outer mitochondrial membrane translocases facing the intermembrane space (IMS) and that this interaction promotes the conformational change needed for full activity. Fractionation assays demonstrate that 3βHSD2 associated with the IMM but did not integrate into the membrane. Through mass spectrometry and Western blotting of mitochondrial complexes and density gradient ultracentrifugation, we show that that 3βHSD2 formed a transient association with the translocases Tim50 and Tom22 and with Tim23. This association occurred primarily through the interaction of Tim50 with the N terminus of 3βHSD2 and contributed to enzymatic activity. Tim50 knockdown inhibited catalysis of dehydroepiandrostenedione to androstenedione and pregnenolone to progesterone. Although Tim50 knockdown decreased 3βHSD2 expression, restoration of expression via proteasome and protease inhibition did not rescue activity. In addition, protein fingerprinting and CD spectroscopy reveal the flexibility of 3βHSD2, a necessary characteristic for forming multiple associations. In summary, Tim50 regulates 3βHSD2 expression and activity, representing a new role for translocases in steroidogenesis.

Most mitochondrial proteins are encoded by nuclear genes, synthesized as precursors on cytosolic polysomes (1), and imported across the outer (OMM)[3] and inner mitochondrial membranes (IMM) (2–5). Loosely associated protein complexes at the mitochondrial membranes, termed translocases, mediate protein import and sorting. Translocase complexes found at the OMM are called Tom (translocase, outer membrane), whereas those at the IMM are called Tim (translocase, inner membrane) (3, 6, 7). The complexes are not tightly linked to each other, making it difficult to accurately determine the precise mechanism of translocation (7, 8). Most proteins enter the mitochondria via the Tom40 channel. After crossing the OMM, Tim50 of the Tim23 complex receives proteins that contain a presequence. Interaction of Tim50 with the preprotein promotes binding of the presequence to the IMS domain of Tom22 (9). Tim50, anchored in the IMS with one transmembrane helix, has a large C-terminal hydrophobic domain of ~350 amino acids exposed to the IMS (10) that coordinates function by maintaining the permeability barrier (11–13). Indeed, loss of Tim50 leads to a release of mitochondrial cytochrome *c* in cells as well as developmental defects in zebrafish embryos due to increased cell death (14). Tim21, of the Tim23 complex, then binds to Tom22, causing the release of the preprotein and its subsequent entry into the Tim23 channel. Preproteins are then sorted to the IMS or mitochondrial matrix (15, 16).

Steroid hormones, synthesized in adrenal and gonadal tissues, are essential for survival of all animals (17). In steroido-

* This work was supported, in whole or in part, by National Institutes of Health Grant HD057876 (to H. S. B.).
[S] The on-line version of this article (available at http://www.jbc.org) contains supplemental Figs. S1–S3 and Tables ST1–ST3.
[1] Both authors were equal contributors.
[2] Supported by the Anderson Cancer Institute and the Mercer University School of Medicine. To whom correspondence should be addressed: Dept. of Biochemistry, Division of Biomedical Sciences, Mercer University School of Medicine and Memorial University Medical Center, Hoskins Research Bldg., 4700 Waters Ave., Savannah, GA 31404. Tel.: 912-350-1710; Fax: 912-350-1765; E-mail: bose_hs@mercer.edu and bosehi1@memorialhealth.com.

[3] The abbreviations used are: OMM, outer mitochondrial membrane; IMM, inner mitochondrial membrane; IMS, intermembrane space; 3βHSD2, 3β-hydroxysteroid dehydrogenase; DHEA, dehydroepiandostenedione; mCCCP, carbonyl cyanide m-chlorophenyl hydrazine; CMC, critical micelle concentration; AU, arbitrary units.

genic tissues, the cholesterol side-chain cleavage enzyme, P450scc, catalyzes cholesterol to pregnenolone, the precursor of all steroids. The IMM-associated 3β-hydroxysteroid dehydrogenase (3βHSD2) (18) catalyzes the conversion of pregnenolone to progesterone, 17α-hydroxy-pregnenolone to 17α-hydroxy-progesterone, and dehydroepiandostenedione (DHEA) to androstenedione in conjunction with NAD^+ as a cofactor (Fig. 1*A*). Thus, altered 3βHSD activity can have a wide range of effects. Serum levels of DHEA-sulfate increase in women with postmenopausal breast cancer (18, 19). In addition, mutant 3βHSD2 both alters sexual development and leads to a severe salt-wasting crisis resulting in congenital adrenal hyperplasia (17–21).

3βHSD2 has both dehydrogenase and isomerase activities. We hypothesize that the bifunctional activity of 3βHSD2 requires the protein to undergo a conformational change. We propose that 3βHSD2 associates with the IMM or OMM translocases facing the IMS and that this interaction promotes a conformational change leading to the two different enzymatic activities. We found that 3βHSD2 associated with the IMM but did not integrate into it. This likely was the result of the interaction between 3βHSD2 and Tim50, resulting in a transient complex formation of 3βHSD2, Tom22, Tim23, and Tim50. The study demonstrates the flexibility of 3βHSD2, which allowed the protein to interact with the membrane bound domains of Tim50. Cytochrome P450c17, expressed in the endoplasmic reticulum (22–24), catalyzes the conversion of 17-OH pregnenolone to DHEA (Fig. 1*A*) in adrenal and testicular tissues. We show that the absence of Tim50 inhibited the catalysis of DHEA to androstenedione and pregnenolone to progesterone but did not affect the expression of endoplasmic reticulum resident cytochrome P450c17 (22–24). Moreover, restoration of 3βHSD2 expression in the Tim50 knockdown cells via proteasome and protease inhibition did not rescue steroidogenic activity. Thus, the association of 3βHSD2 with the translocase appears to play a key role in the regulation of enzymatic activity.

EXPERIMENTAL PROCEDURES

Isolation and Purification of Mitochondria—Mitochondria were obtained from cell lines or, as a control, from pig adrenal glands. The pig adrenals were excised immediately after animal sacrifice at the Department of Animal Sciences, University of Florida. The adrenal tissues were diced in mitochondrial isolation buffer (250 mM sucrose, 10 mM HEPES, 1 mM EGTA, pH 7.4), whereas the cell lines were washed with PBS two times and then incubated with 1 mM HEPES, pH 7.4, for 30 min at 4 °C. Next, tissues and cells were homogenized in a hand-held all-glass Dounce homogenizer with 40 gentle up and down strokes, and the cell debris was removed by spinning at 3500 × *g* for 10 min. The supernatant containing the mitochondrial fraction was purified by differential centrifugation following a previously reported procedure (25, 26), and the pellet was washed and then resuspended in an energy regeneration buffer (125 mM sucrose, 80 mM KCl, 5 mM $MgCl_2$, 10 mM NaH_2PO_4, 10 mM isocitrate, 1.0 mM ATP, 1.0 mM NADP, 0.1 mM ADP, and 25 mM HEPES, pH 7.4) before storage at either −86 °C or in liquid nitrogen.

Protein Import—To synthesize [^{35}S]methionine labeled proteins, the cDNAs for 3βHSD2 and the COX IV dihydrofolate reductase fusion were subcloned into the SP6 vector, and proteins were synthesized in a cell-free system in the presence of [^{35}S]Met using TNT-rabbit reticulocyte (Promega). Ribosomes and associated incompletely translated polypeptide chains were removed by centrifugation at 150,000 × *g* for 15 min at 4 °C (27). For all protein import experiments, a 100-μl mixture of isolated mitochondria (100 μg) and synthesized protein was incubated in a 26 °C water bath with or without proteinase K, and the import reaction was terminated by the addition of 1 mM mCCCP and an equal volume of boiling 2× SDS sample buffer. The import reactions were analyzed by electrophoresis through SDS-polyacrylamide gels, fixing the gels in methanol/acetic acid (40:10), and then drying and exposing gels to a phosphorimaging screen.

Native Polyacrylamide Gel Electrophoresis (PAGE)—To analyze complex formation, ^{35}S-labeled 3βHSD2 was incubated with mitochondria isolated from MA-10 cells, and the reaction was stopped by placing the mix on ice. Membranes were then lysed with buffer containing digitonin, and the samples were electrophoresed through 3–16% gradient native gels. In some cases gels were fixed, dried, and then exposed to phosphorimaging In other cases protein complexes were transferred to a membrane and then probed with antibodies against 3βHSD2, Tom22, Tim50, or Tim23.

Mitochondrial Fractionation—The mitochondrial compartments were individually purified following a standard procedure with minor modifications. In brief, the OMM fraction was extracted with 1.2% digitonin, and the remaining mixture of matrix and IMM was purified through 0.5% Lubrol, where the matrix fraction remained in solution after centrifugation, and the IMM fraction formed the pellet (28). Proteins with a nonspecific association or loose association with the membranes were removed by incubation with proteinase K. Fractions were then processed for Western blotting using the indicated antibodies.

Proteolytic Digestion—Limited proteolytic digestion experiments were performed at room temperature or 4 °C using 5 μg of 3βHSD protein and different concentrations of trypsin (sequencing grade, Promega) for either 15 or 45 min. The reactions were terminated by adding of an equal volume of SDS-sample buffer containing 2 mM PMSF and then incubating in a boiling water bath. After electrophoresis, the samples were stained with Coomassie Brilliant Blue or silver nitrate.

Liquid Chromatography Mass Spectrometry (LC-MS/MS)—Complexes were excised, destained, reduced with DTT (Roche Applied Science), alkylated with iodoacetamide (Sigma), and then digested with trypsin (Promega Sequencing Grade Modified) overnight (29). The extracted peptides were analyzed by mass spectrometry via LC-MS/MS on a nanoAcquity UPLC (Waters, MA) coupled with a Q-TOF-Premier mass spectrometer (Micromass, UK/Waters, MA). Tryptic peptides were separated using a linear water/acetonitrile gradient (0.1% formic acid) on a nano Acquity column (3-μm Atlantis dC18, 100 Å pore size, 75-μm inner diameter × 15 cm) (Waters, MA) with an in-line Symmetry column (5-μm C18, 180-μm inner diameter × 20 mm) (Waters, MA) as a loading/desalting column.

Protein identification using the generated MS/MS spectra was performed by searching the NCBI non-redundant data base using Mascot MS/MS Ion Search at Matrix Science with consideration for the carbamidomethylation of cysteine and the oxidation of methionine.

Density Gradient Ultracentrifugation—Complexes were resolved by a sucrose density gradient (top 10% to bottom 30%) with a cushion of 200 μl of 68% (2.0 M) sucrose in a final volume of 2 ml. Approximately 100 μg of protein in a volume of 100 μl was layered on the top and centrifuged at 4 °C in a Beckman TLA55 rotor at 55,000 rpm for 1 or 4 h. After centrifugation, fractions of 125 μl were collected. Gradient fractions were analyzed by native PAGE to show that the complexes were not degraded during centrifugation through the sucrose density gradient. Fractions were subjected to immunoprecipitation to determine specific interactions. An aliquot of 20 μl of each fraction was electrophoresed on a 15% SDS-polyacrylamide gel, and the components were analyzed by Western blot.

siRNA Knockdown Experiments and Generation of Tim50 Knockdown Cell Lines—siRNA (5′-GGGACATCATGTGAAGGACtt-3′) and (5′-GGACATCTCCTGTCTGAATtt-3′) for Tim50, (5′-GCCAGTCTGGAGTTGCTTTtt-3′) and (5′-CGCTATCTCGTTCAGGATAtt-3′) for Tim23, and (5′-GAAGATGTACAGATTTTCCtt-3′) and (5′-CCTTGGCACATGGATCTATtt-3′) for Tom22 were obtained from Ambion/Invitrogen. COS-1 and MA-10 cells were transfected with 30 and 60 pmol of siRNA, respectively, using Oligofectamine (Invitrogen). Non-targeting siRNA as well as a combination of two non-targeting scrambled siRNAs (Ambion) were included as controls in all experiments. The pSilencer siRNA expression plasmid for Tim50 was constructed by ligating the 55-mer siRNA template into a pSilencer 4.1 CMV expression vector (Ambion). Complementary 55-mer siRNA oligonucleotides (5′-GATCGGACATCATGTGAAGGACTTCAAGAGAGTCCTTCACATGATGTCCCTTTTTTAGGAAA-3′ and 3′-GCCCUGTAGUACACTTCCTGAAGTTCTCTAACTATGGACCCAGGAAGTGTACTACAGGGAAAAAACCTTTTCGA-5′) were annealed, ligated into pSilencer neovector (Ambion), and transformed into competent *Escherichia coli* to screen for positive hairpin siRNA inserts. The accuracy of the knockdown was determined by Western blotting. For generation of stable cell lines, COS-1 and MA-10 cells were independently transfected with the purified plasmid using Lipofectamine (Invitrogen). Single clones were generated 48 h after transfection by limiting dilution into a selection medium containing 600 mg/ml G418 (Geneticin). Individual clones were then transferred to 24-well plates (Greiner) for propagation and then later transferred to 6-cm plates for transfection. Individual clones were examined for Tim50 expression by Western blotting. Western blotting was performed with 12.5 mg of protein and with specific primary antibodies. Signals were developed with West-Pico chemiluminescent reagent (Pierce).

Co-immunoprecipitations—Specific antibodies were preincubated with protein A-Sepharose CL-4B (0.5 μg/μl, GE Healthcare) in 100 μl of 1× co-immunoprecipitations buffer (1% Triton X-100, 200 mM NaCl, and 0.5% sodium deoxycholate) for 2 h at 4 °C. To remove unbound antibody, beads were washed with 1× co-immunoprecipitations buffer and then incubated with a rabbit IgG control antibody (Sigma) for 1 h to block unbound beads and then washed. The freshly isolated mitochondrial pellet (25 mg for each sample) was resuspended with ice-cold lysis buffer (20 mM Tris HCl pH 8.0, 137 mM NaCl, 10% glycerol, 1% Triton X-100, 2 mM EDTA), and unsolubilized material was removed by ultracentrifugation (30 min at 100,000 × *g*). The supernatants were incubated with antibody-bound protein A-Sepharose beads overnight at 4 °C. After washing, the protein A-Sepharose pellets were resuspended in 100 mM glycine, pH 3.0, for 10 s, and then a pretitrated volume of 1.0 M Tris, pH 9.5, was added to adjust the pH to 7.4. Immune complexes were then analyzed by Western blotting.

Metabolic Conversion Assays—Isolated mitochondria (300 μg) were incubated in potassium phosphate buffer for the conversion of [^{3}H]pregnenolone to progesterone. Three million counts of [^{3}H]pregnenolone were used for each reaction and chased with 30 μg of cold unlabeled progesterone. The reaction was initiated by the addition of NAD and incubated at 37 °C for 4 h in a shaking water bath. To measure the conversion of DHEA to androstenedione, mitochondria were incubated with 80,000 counts of [^{14}C]DHEA, and the reaction was initiated by the addition of NAD and incubated as above. For some of the experiments, protease or proteasome inhibitors were included. For both reactions, the steroids were extracted with ether/acetone (9:1 v/v), and equal amounts of a cold pregnenolone-progesterone (50:50, Sigma) mixture in CH_2Cl_2 were added as a carrier. The extracts were concentrated under a stream of nitrogen or air and then separated by TLC (Whatman) using a chloroform/ethyl acetate (3:1) mobile phase. The radioactivity was enhanced using [^{3}H]Enhancer, and the amounts of each steroid were determined using phosphorimaging.

Gas Chromatography-Mass Spectrometry (GCMS)—The spots extracted from TLC plates were subjected to GCMS analysis on an Agilent 7890 GC with 5975C mass spectrometer. The column used was an Agilent HP-5 with dimensions 30-m × 0.25-mm inner diameter with a 0.25-μm film thickness. Samples were dissolved in 50 μl of dichloromethane, and 1 μl was injected onto the column using a pulsed splitless injection. The temperature program was as follows: ramp at 10 °C/min from 70 to 310 °C and hold for 6 min. Spectra were collected in full scan mode over the mass range m/z 50–500 to facilitate comparison of MS spectra with the NIST/EPA/NIH NIST08 mass spectral library.

Detergent Exchange of Purified 3βHSD2 Using Hydroxylapatite Chromatography—Human 3βHSD2 was purified from mitochondria of recombinant baculovirus-infected Sf9 cells (30) using DEAE ion-exchange chromatography in the presence of Igepal CO-720 detergent (Rhodia, Inc., Cranbury, NJ) as previously described (31). The low critical micelle concentration (CMC) Igepal detergent was exchanged for the high-CMC detergent, Cymal-5 (Anatrace, Inc., Maumee, OH), using hydroxylapatite chromatography. The 3βHSD2 fraction pool from the DEAE column was applied to the hydroxylapatite column (1 mg of protein/ml of packed gel), washed with 3.5 column volumes of 0.025 M potassium phosphate, pH 7.5, 20% glycerol, 0.1 mM EDTA, 0.01 M NAD, 1.8 mM Cymal-5, and eluted with 0.30 M

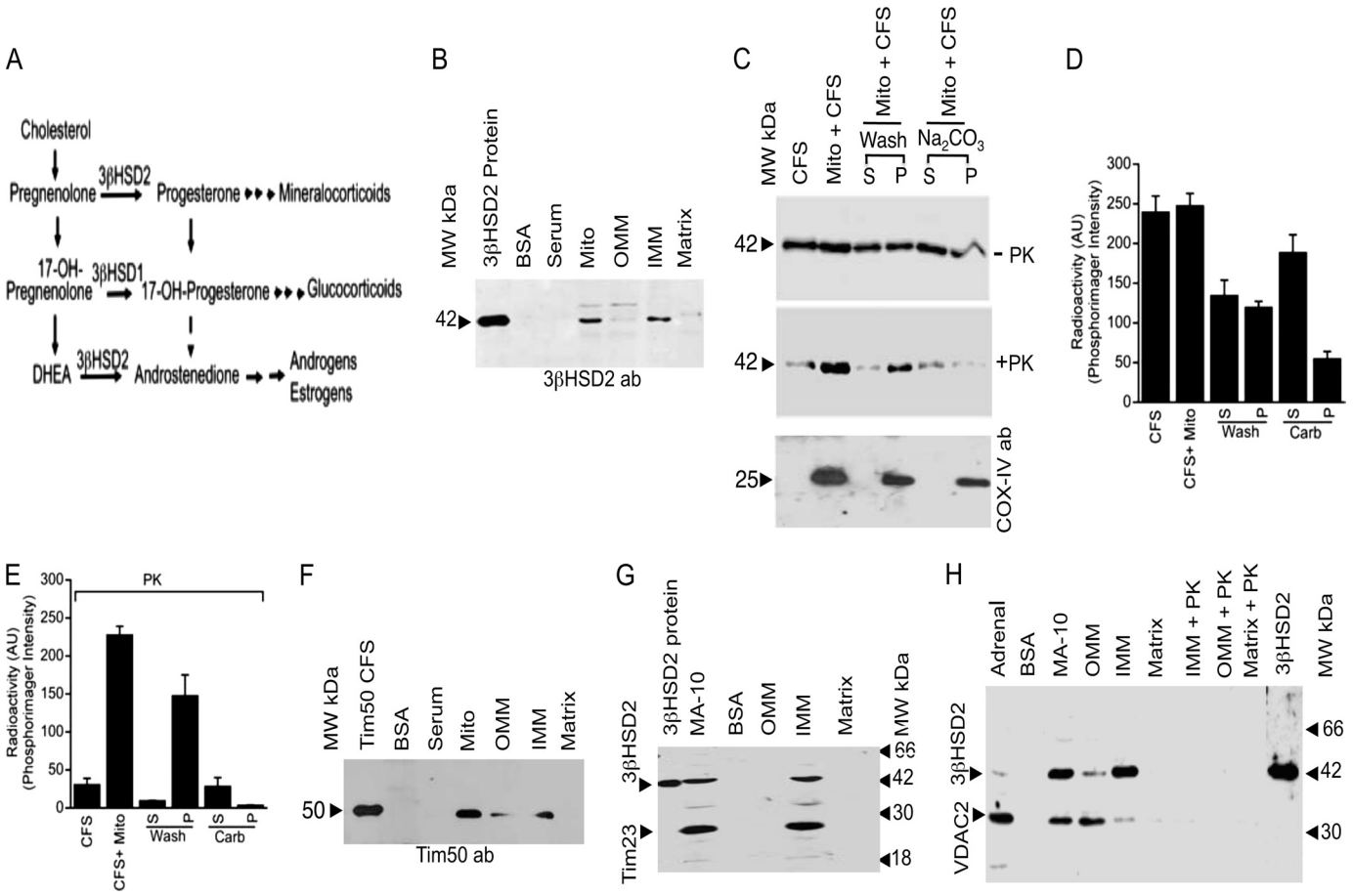

FIGURE 1. **Compartment-specific location of 3βHSD2.** *A*, shown is a schematic representation of the steroid hormone synthesis pathway and the role of 3βHSD2. *B*, shown is a Western blot of mitochondrial (*Mito*) fractions from MA-10 cells probed with 3βHSD2 antibodies. 3βHSD2 was associated with the IMM fraction. *C*, mitochondrial import of cell-free synthesized (*CFS*) ^{35}S-labeled 3βHSD2 is shown. After incubation of ^{35}S-labeled 3βHSD2 with isolated mitochondria, the imported (*P*) fraction was separated from non-imported fraction (*S*) by washing. In some cases fractions were extracted with Na_2CO_3. Fractions were briefly treated with (*middle panel*) or without protein kinase (*PK*, *top panel*). After electrophoresis, gels were fixed and dried. Gels were also processed for Western blotting using an antibody directed against COX IV (*bottom panel*). *D* and *E*, quantitation of bands was done using phosphorimaging. Data are presented as the mean ± S.E. of three independent experiments. Although not an integral protein, 3βHSD2 specifically associates with IMM; *WASH*, washing; *CARB*, carbonate. *F–H*, shown are Western blots of MA-10 mitochondrial compartments using antibodies directed against Tim50 (*F*), Tim23 and 3βHSD2 (*G*), and VDAC2 and 3βHSD2 (*H*).

potassium phosphate, pH 7.5, 20% glycerol, 0.1 mM EDTA, 0.01 M NAD, 1.8 mM Cymal-5. The peak of 3βHSD2 activity was pooled and found to be free of Igepal CO-720 based on absorbance at 280 nm due to the Igepal CO-720.

RESULTS

3βHSD2 Is an IMM-associated Protein—The specific location of 3βHSD2 within the mitochondria is not yet known. Thus, we did fractionation studies using isolated mitochondria from mouse Leydig MA-10 cells and found 3βHSD2 localized to the IMM (Fig. 1*B*). The size of the 3βHSD2 associated with the IMM fraction appeared similar to that of the control 3βHSD2 purified from baculovirus, indicating that the protein did not undergo signal sequence cleavage. We then evaluated if 3βHSD2 integrates into the IMM or if it merely associates with the membrane by performing import assays with cell-free-synthesized ^{35}S-labeled 3βHSD2 and isolated mitochondria from MA-10 cells (Fig. 1, *C–E*). We separated the non-imported (*S*) from the imported fraction (*P*) by centrifugation and analyzed membrane integration by extracting the pellet with Na_2CO_3. Sodium carbonate breaks protein-protein interactions but not lipid-protein interactions (3). Although the identical size of ^{35}S-labeled 3βHSD2 before and after import suggests an uncleaved N terminus, a common characteristic for IMM proteins, our observation that 3βHSD2 returned to the supernatant after carbonate extraction indicates that the protein was not integrated into the IMM. A brief incubation with a protease results in the digestion of proteins with a nonspecific membrane association as the enzyme cannot enter the membrane. Thus, the fact that incubation of fractions with proteinase K only ablated signal in the non-imported fractions suggests that a specific association between 3βHSD2 and the IMM. As a control, we evaluated each fraction for the presence of COX IV, an integrated IMM protein facing the matrix. The Western blots validated the mitochondrial integrity during fractionation, extraction, and proteolysis (Fig. 1*C*). In summary, the results confirm that 3βHSD2 was imported like a typical inner membrane protein and suggest that 3βHSD2 may specifically associate with the IMM without integration into the membrane.

To determine the compartment specific localization of 3βHSD2 at the IMM, we performed Western analysis on mitochondrial fractions from steroidogenic MA-10 cells and

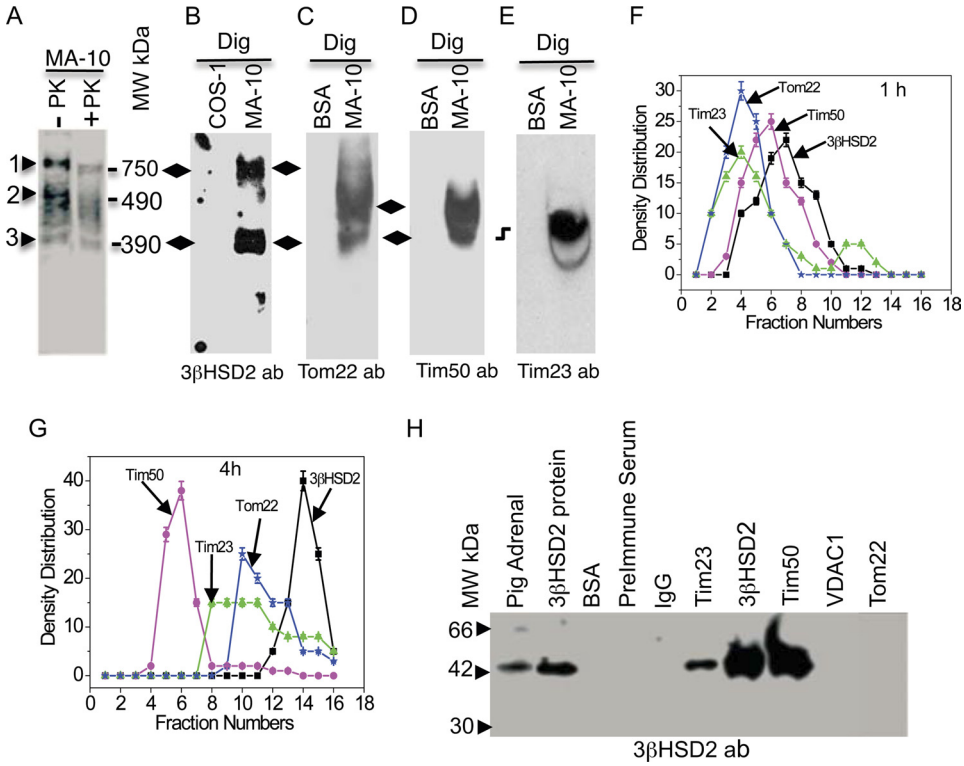

FIGURE 2. **Association of 3βHSD2 with mitochondrial translocases.** *A*, ^{35}S-labeled 3βHSD2 was imported into isolated mitochondria, and the digitonin (*Dig*)-solubilized fraction was analyzed through native gradient gel electrophoresis. 3βHSD2-containing complexes were identified at 750, 490, and 390 kDa. *PK*, protein kinase. *B–E*, shown are Western blots of the native-page complexes probed with antibodies directed against 3βHSD2, Tom22, Tim50, and Tim23. *F* and *G*, sucrose density gradient analysis of the digitonin-lysed mitochondrial complex after 1 (*F*) and 4 (*G*) h of ultracentrifugation is shown. Each fraction was probed with the indicated antibodies, and the distribution of the proteins was graphed. Data presented are the mean ± S.E. of three independent experiments. The graphs indicate that 3βHSD2 was associated for a limited time of 1 h with all the translocases. *H*, shown are co-immunoprecipitation using isolated mitochondria from MA-10 cells and the indicated antibodies (*ab*) followed by Western blotting with the 3βHSD2 antibody. 3βHSD2 directly interacted with Tim23 and Tim50.

included antibodies directed against proteins known to localize in the IMM or OMM. We found that the IMM fraction contained both Tim50 and Tim23 (Fig. 1, *F* and *G*). To confirm that we successfully separated the OMM from the IMM, we probed fractions for the presence of voltage dependent anion channel (VDAC2), an OMM protein, and saw that VDAC2 primarily localized to the OMM (Fig. 1*H*). 3βHSD2 was seen in the IMM fractions (Fig. 1, *G* and *H*). Similarly, 3βHSD2 also localized to the IMM in human breast cancer MCF-7 cells and human adrenal NCI H295 cells (data not shown).

3βHSD2 Is Associated with Tim50 and Tom22—From the above studies we found that 3βHSD2 specifically associated with the IMM but was not integrated into the membrane (Fig. 1, *B–E*). This association with the IMM led us to evaluate what proteins 3βHSD2 may bind to in the mitochondria. We did import assays using cell-free-synthesized ^{35}S-labeled 3βHSD2 and mitochondria isolated from steroidogenic MA-10 cells. Samples were treated with proteinase K to proteolyze non-specifically associated proteins. Digitonin lysis of the imported ^{35}S-labeled 3βHSD2 and subsequent native gradient gel electrophoresis resulted in the appearance of three 3βHSD2-containing complexes, 750, 490, and 390 kDa in size (Fig. 2*A*). The two smaller complexes may represent a breakdown from the larger complex, but resistance to proteinase K suggests tightly associated protein complexes. LC-MS/MS analysis of the major 750-kDa complex revealed several mitochondrial proteins (supplemental Table ST1), including outer membrane translocase Tom22, inner membrane translocase Tim50, and 3βHSD2. These results suggest that the outer and inner mitochondrial translocases may coordinate their functions through 3βHSD2.

Tranlocases help ensure the proper localization of mitochondrial proteins. Most mitochondrial proteins, synthesized as precursor proteins in the cytosol (3, 5, 6, 32), enter the mitochondria through Tom40, a translocase complex at the OMM (3, 6). Proteins then reach their final destination within the mitochondria through the action of additional translocase complexes. For example, Tim23 at the IMM directs proteins with a presequence to either the IMM or matrix. Each translocase complex consists of multiple proteins that can transiently associate with proteins in other complexes (7, 8). Tim50, a component of the Tim23 complex, binds to proteins emerging from the Tom40 channel and stimulates interaction between the presequence and Tom22 (9). Tim21, another component of Tim23 (11), competes with the presequence for binding to Tom22 and thereby causes the release of the protein and its subsequent translocation through the Tim23 channel.

To validate that 3βHSD2 associates with translocases, we performed Western analysis of the native complexes using antibodies directed against 3βHSD2, Tom22, Tim50, and Tim23 (Fig. 2, *B–E*). We included Tim23 antibodies, as others have shown that IMM resident Tim50 (supplemental Fig. S2e) asso-

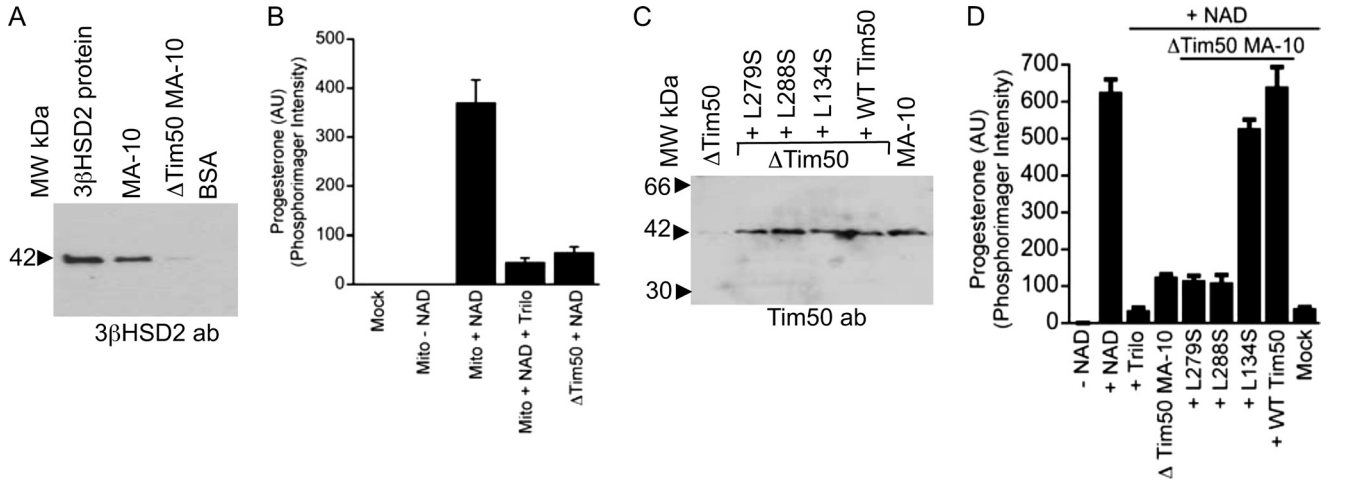

FIGURE 3. **Role of Tim50 in progesterone synthesis.** *A*, shown is expression of 3β*HSD2* in ΔTim50 MA-10 cells. Baculovirus-purified 3β*HSD2* served as a control. *ab*, antibody. *B*, shown is metabolic conversion of [^{3}H]pregnenolone to [^{3}H]progesterone using mitochondria (*Mito*) from ΔTim50 MA-10 cells. The addition of NAD initiated the reaction, whereas trilostane inhibited 3β*HSD2* activity. Tim50 knockdown resulted in a 7-fold decrease in progesterone synthesis. Data presented are the mean ± S.E. of three independent experiments. *C*, expression of wild-type and indicated mutant Tim50 cDNAs in ΔTim50 cells was determined by Western blotting with a Tim50 antibody. Transfection with mutant or wild-type Tim50 restored expression in knockdown cells. *D*, shown is metabolic conversion of [^{3}H]pregnenolone to [^{3}H]progesterone in Tim50 knockdown cells transfected with mutant or wild-type Tim50. Tim50 mutants L279S and L288S displayed similar levels of activity as knockdown cells, but wild-type Tim50 and mutant L134S restored the metabolic conversion. Data presented are the mean ± S.E. of three independent experiments.

ciates with flexible Tim23 (10) to coordinate the function of mitochondrial protein by maintaining a permeability barrier (11–13). We indeed observed all four proteins in the 390-kDa complex, whereas the 490-kDa complex contained only Tim50 and Tom22, and the 750-kDa complex contained only 3β*HSD2* and Tom22 (Fig. 2, *B–E*). It is possible that Tim23 was not identified in the MS analysis because of the higher abundance of other proteins. The observation that Tom22 localized to all three complexes may be because its C terminus faces the IMS side of the IMM, whereas the majority of the protein is associated with the OMM. The minor association of Tom22 with the 750-kDa complex is possibly due to a loose association with 3β*HSD2* (Fig. 2*C*). The lack of 3β*HSD2* detection in the 490-kDa complex suggests an association of the Tim50 emerging at the trans side of the Tom channel and promoting binding of the presequence to the Tom22 IMS domain, resulting in a direct interaction between 3β*HSD2* and Tom22. Alternatively, the lack of 3β*HSD2* in the 490-kDa complex may indicate that it was buried within the native complex. As a result, the association between Tim50 and 3β*HSD2* was likely to be transient and, thus, flexible enough to coordinate interaction with Tom22. In summary, the different sizes and components of the native complexes support the notion that 3β*HSD2* participates in the fluid and transient associations that form between the different translocases (7, 8).

These experiments clearly indicate that 3β*HSD2* and the three translocases form a network that connects the OMM and IMM. To further demonstrate that these proteins remain closely localized in the mitochondria, we purified digitonin-lysed mitochondria through a sucrose density gradient and then examined the fractions by Western blotting (Fig. 2, *F* and *G*). During a longer separation (4 h), Tim23 and Tom22 appeared closely associated as they co-localized in fractions 8–12, whereas Tim50 and 3β*HSD2* were more distantly separated (Fig. 2*G*), suggesting a weak interaction between 3β*HSD2* and the translocases. However, during a shorter separation (1 h), 3β*HSD2* showed an overlapping distribution with Tim23, Tim50, and Tom22 (Fig. 2*F*), suggesting the interaction of all four proteins. The interactions may not have been of equal strength, however, as the distribution of 3β*HSD2* more closely mirrored that of Tim50 than Tom22 (Fig. 2*F*). Indeed, co-immunoprecipitation with the translocase antibodies followed by Western blotting for 3β*HSD2* demonstrated that 3β*HSD2* interacted strongly with Tim50, weakly with Tim23, but not with Tom22 (Fig. 2*H*). Taken together, it seems that 3β*HSD2* and Tim50 specifically interact, and through this interaction 3β*HSD2* associates with the other translocases transiently.

Tim50 regulates progesterone and androstenedione synthesis- We next evaluated if the interaction between Tim50 and 3β*HSD2* had a biological effect by knocking down Tim50 (ΔTim50) in steroidogenic MA-10 cells and measuring the metabolic conversion of pregnenolone to progesterone. siRNA reduced 3β*HSD2* expression by 90% (Fig. 3*A*, supplemental Fig. S2*a*) and mitochondria from these cells produced 65 ng/ml progesterone as compared with 370 ng/ml from control cells (Fig. 3*B*, supplemental Fig. S2*b*). We also performed rescue experiments by transfecting ΔTim50 cells with expression vectors for either wild-type or mutant Tim50. The IMS domain of Tim50 lies between amino acids 133–476 and is indispensible for Tim50 interaction with Tim23; thus, we generated two Tim50 mutants in this domain, L279S and L288S. The endo group reported that these mutants had reduced interactions with Tim23 (11). We also generated the mutant L134S to evaluate the effect of a conformational change at the beginning of the IMS domain. Wild-type and mutant Tim50 vectors expressed approximately the same level of Tim50 protein (Fig. 3*C*). However, only wild-type Tim50 and L134S rescued progesterone synthesis (Fig. 3*D*, supplemental Fig. S2*c*). Studies have shown that point mutations in Tim50 reduce activity that is likely related to the degree of conformation change of the protein

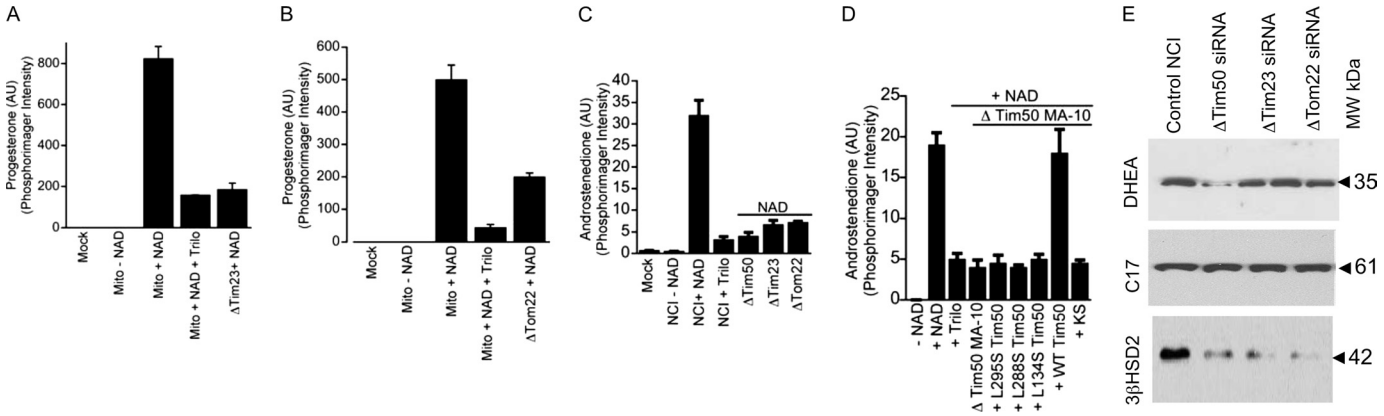

FIGURE 4. **Role of Tim23, Tim50, and Tom22 in conversion of pregnenolone and DHEA.** *A* and *B*, conversion of [^{3}H]pregnenolone to [^{3}H]progesterone in ΔTim23 cells (*A*) and ΔTom22 (*B*). As compared with control cells, ΔTom22 mitochondria produced 63% less progesterone whereasΔTim23 mitochondria produced 60% less. *C*, shown is metabolic conversion of DHEA to androstenedione after knockdown of Tim50, Tim23, and Tom22 in human adrenal NCI H295 cells. DHEA to androstenedione was significantly reduced in ΔTim50 cells as compared with ΔTim23 and ΔTom22 cells. *D*, shown is measurement of DHEA to androstenedione in ΔTim50 cells transfected with wild-type or mutant Tim50 cDNA. Tim50 knockdown ablated the conversion of DHEA to androstenedione, and only expression of wild-type Tim50 could rescue the enzymatic activity. Plasmid Bluescript KS is an internal negative control. *E*, shown is expression of DHEA, P450c17, and 3β*HSD2* in control NCI H295, ΔTim50, ΔTim23, and ΔTom22 cells as determined by Western blot. DHEA expression was decreased in ΔTim50 cells without affecting its precursor, P450c17.

(11). Mutation in steroidogenic proteins can be lethal for human survival (17, 33). Thus, Tim50 mutants may be misfolded and unable to interact with 3β*HSD2*, resulting in the loss of 3β*HSD2* activity.

Because Tim23 also associated with 3β*HSD2* and Tim50, we knocked down Tim23 expression with siRNA (ΔTim23) in steroidogenic MA-10 cells (supplemental Fig. S3*a*) and determined 3β*HSD2* activity. As expected, Tim23 siRNA reduced conversion of pregnenolone to progesterone by 63% (Fig. 4*A*), suggesting that Tim23 contributes to 3β*HSD2* activity.

Two current models (11, 12) suggest that the Tom22 C terminus faces Tim50, so Tom22 may interact transiently with 3β*HSD2*. Moreover, 3β*HSD2* charge segments may provide binding sites for presequence-carrying preproteins traversing the OMM and IMM (34). Thus, we also evaluated the effect of Tom22 knockdown. In ΔTom22 cells, 3β*HSD2* expression was reduced 80% as compared with wild-type cells (supplemental Fig. S3*b*). Progesterone synthesis was also reduced, from 503 to 190 ng/ml (Fig. 4*B*), indicating an indispensible role for Tom22 in 3β*HSD2* activity. Perhaps the 62% reduction in progesterone synthesis resulted from the loss of the weak interaction between 3β*HSD2* and Tom22 because Tom22 binds preproteins through both its cytosolic domain and intermembrane space domain, which is stably associated with the channel protein Tom40 (35) that has a significant C-terminal domain at the IMS (36, 37).

3β*HSD2* also converts DHEA to androstenedione; thus, we explored the effect of translocase knockdown on this activity. Rodents do not convert DHEA directly to androstenedione, so for this experiment we used human adrenal NCI H295 cells and found that knockdown of Tom22, Tim23, and Tim50 resulted in a similar level of androstenedione synthesis as treatment of cells with the 3β*HSD2* inhibitor, trilostane (Fig. 4*C*). Again, in ΔTim50 cells, wild-type Tim50 restored androstenedione synthesis (Fig. 4*D*); however, none of the Tim50 mutants, including L134S, restored activity (Fig. 4*D*, supplemental Fig. S3c).

Tim50 Coordinates in Specific Steps of Steroidogenesis—We next evaluated the expression of P450c17 in the knockdown cells. This enzyme is responsible for converting pregnenolone and progesterone to their 17-hydroxy forms (Fig. 1*A*) and then converting these to DHEA and androstenedione. P450c17 plays a crucial role in DHEA expression as the 17,20 lyase activity is about 50 times more efficient for the conversion of 17α-hydroxypregnenolone to DHEA than for the conversion of 17α-hydroxyprogesterone to androstenedione (Fig. 4*E*, *middle panel*). Fig. 4*E* shows that the expression level of P450c17 (*middle panel*) remained the same between control and knockdown cells. However, DHEA showed a marked decrease in ΔTim50 cells (*top panel*), whereas 3β*HSD2* expression was nearly ablated in all the knockdown cells (*bottom panel*). These results suggest that defects in DHEA conversion were due solely to 3β*HSD2*, although the role of Tim50 in DHEA synthesis requires further investigation.

The possibility exists that the decrease in 3β*HSD2* expression seen in cells with ΔTim23 and ΔTom22 knockdown was due to the misfolding and subsequent proteolysis by IMS resident proteases of unused 3β*HSD2*. To test this possibility, we incubated ΔTim50 cells with increasing concentrations of protease and proteasomal inhibitors and determined 3β*HSD2* expression (supplemental Fig. S3*d*). The expression of 3β*HSD2* was restored with the cysteine protease inhibitor, E64, and proteasomal inhibitor lactacystin (Fig. 5*A*). However, restoration of 3β*HSD2* expression did not rescue the conversion of pregnenolone to progesterone (Fig. 5*B*) or DHEA to androstenedione (Fig. 5*C*), confirming that the presence of Tim50 is mandatory for 3β*HSD2* activity.

Flexibility of 3βHSD2 Helps in the IMM Network—Given the multiple interactions of 3β*HSD2* with the different translocases, the protein is likely flexible. To address this possibility, we performed protein fingerprinting of baculovirus-expressed 3β*HSD* protein. We incubated the protein with trypsin for 15 or 45 min at two temperatures to identify domains that are differentially protected from proteolysis. For flexible proteins, lysine and arginine residues will be exposed to trypsin, generating proteolysis to smaller fragments. Trypsin treatment of 3β*HSD* for 45 min at 4 °C resulted in one protected band (Fig.

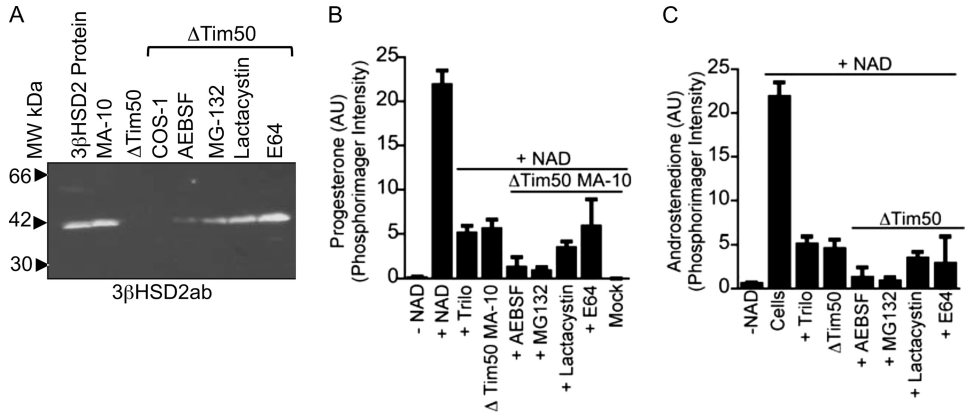

FIGURE 5. **Presence of Tim50 is essential for steroidogenic activity.** *A*, a Western blot of ΔTim50 MA-10 cells shows restored 3βHSD2 expression to a greater extent with E64 than lactacystin, MG132, and 4-(2-aminoethyl)benzenesulfonyl fluoride (*AEBSF*). *B* and *C*, measurement of pregnenolone to progesterone and DHEA to androstenedione conversion using mitochondria from ΔTim50 cells that were treated with the indicated inhibitors is shown. Although lactacystin and E64 restored 3βHSD2 expression, the inhibitors did not restore 3βHSD2 activity in ΔTim50 cells. *Trilo*, trilostane.

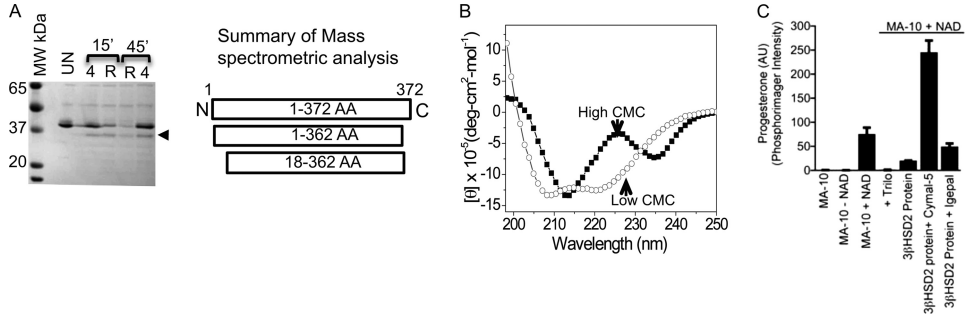

FIGURE 6. **Secondary structural characterization and membrane association of 3βHSD2 protein.** *A*, shown is proteolytic digestion of the purified 3βHSD protein. After trypsin digestion of 5 μg of protein for 15 and 45 min at 4 °C or room temperature (*R*), the samples were electrophoresed on a 22% acrylamide gel and stained with Coomassie Blue. The protected bands, indicated with an *arrowhead*, were excised for mass spectrometric analysis. The photograph understates the differences in staining intensity in the original gels; the indicated bands are decidedly more prominent than others. The *right-hand panel* summarizes the region of amino acids identified by mass spectrometry. *UN*, untreated. *B*, conformational analysis of 3βHSD2 purified from baculovirus by circular dichroism from 200–250 nm with minima at 208 and 222 nm, indicating a mixture of more α-helix than β-sheet conformation. *C*, shown is metabolic conversion of pregnenolone to progesterone in MA-10 mitochondria after the addition of 3βHSD2 protein with and without detergents of lower (Cymal-5) and higher (Igepal CO-720) critical micelle concentration. Data presented in *panels B* and *C* are the mean ± S.E. of three independent experiments.

6*A*). LC-MS/MS analysis of this band identified sequence matching the N-terminal 18–362 amino acids of the wild-type protein (supplemental Tables ST2 and ST3), indicating no protection of bands in 3βHSD2 (Fig. 6*A*, *right-hand panel schematic*).

We next used CD spectroscopy to further evaluate the flexibility of 3βHSD2. This technique can determine conformational changes with minor variations and distinguish secondary structural components with a minima at 198–204 nm indicating random coils, at 208 nm and 222 nm indicating ***α***-helices, and 218 nm indicating β-sheets (38, 39). Computational analysis suggests 3βHSD2 is a mixture of α and β: 32% α-helix, 18% β-sheet, and 50% turn (Fig. 6*B*). In the presence of the low CMC detergent, Cymal-5, 3βHSD2 exhibited a α/β conformation that changed to a more flexible β-turn (Fig. 6*B*, *black square*) in the presence of the high CMC detergent, Igepal CO-720. Smaller proteins or shorter peptides with more β-turn have higher substrate activity as compared with proteins with less or no β-turn (40). Although we observed a direct relationship between 3βHSD2 activity and protein concentration, we also noted that the addition of detergent with low CMC increased activity (supplemental Fig. S3*g*). The activity of 3βHSD2 was 5-fold higher with Cymal-5, (detergent with lower CMC) (Figs. 6*C* and supplemental Fig. S3*g*) than with Igepal-CO-720 (detergent with higher CMC). This experiment strongly suggests that the lower CMC detergent created conditions similar to those in the inner mitochondrial space, and thus 3βHSD2 reaches the appropriate conformation while associated with the translocases, supporting the likelihood that 3βHSD2 is a flexible protein.

N-terminal Amino Acid Sequence Is Responsible for Interaction with Translocases—To understand the mechanism of interaction between 3βHSD2 and the amino acids connecting Tim50 and Tom22, we designed experiments to determine those specific regions of 3βHSD2 responsible for interaction with the translocases using native gradient gel electrophoresis. We made deletion constructs from the N terminus and the C terminus by deleting amino acids in increments of three at a time but keeping the first N-terminal methionine. Import of the cell-free-synthesized deletion mutants into isolated mitochondria followed by digitonin lysis and electrophoresis in native gradient PAGE showed that 3βHSD2 lacking the first three amino acids (from amino acids 2–5 generating Δ2–5 3βHSD2) did not form a 750-kDa complex (Fig. 7*A*), suggesting that the first three amino acids are essential for import into mitochondria. However, mitochondrial import, fractionation, and

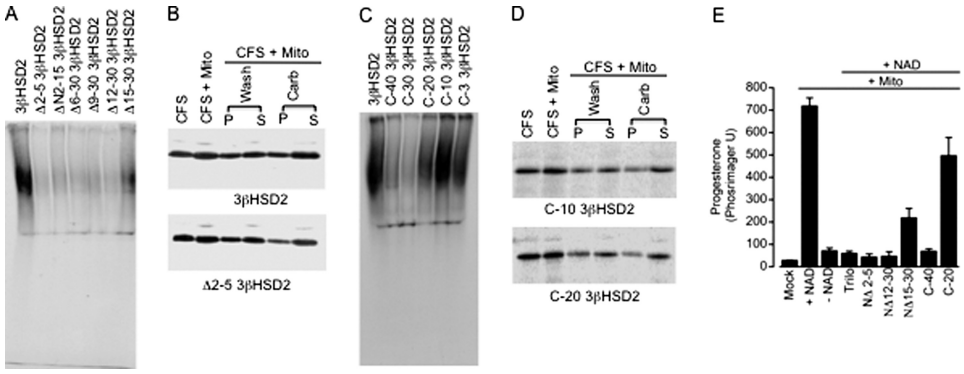

FIGURE 7. **3βHSD2 acts at the IMM directionally.** *A*, different N-terminal ^{35}S-labeled 3βHSD2 deletion mutants, as indicated, were imported into isolated mitochondria (*Mito*), and the digitonin-solubilized fraction was analyzed through native gradient gel electrophoresis. N-terminal 15 amino acids are essential for interaction with the membrane. *B*, import and fractionation of wild-type (*top panel*) and NΔ2–5 ^{35}S-labeled 3βHSD2 (*bottom panel*) after import into the isolated mitochondria are shown. After incubation of ^{35}S-labeled 3βHSD2 with isolated mitochondria, the imported (*P*) fraction was separated from non-imported fraction (*S*) by washing (*WASH*) and also by extraction with Na_2CO_3 (*CARB*). The result shows most of the fraction was remained in the supernatant (*S*) than in pellet (*P*) fraction after extraction with sodium carbonate. Thus, both the wild-type and mutant was processed into the mitochondria in a similar fashion. *C*, the indicated C-terminal ^{35}S-labeled 3βHSD2 mutants were imported into isolated mitochondria, and the digitonin-solubilized fraction was analyzed through native gradient gel electrophoresis in a similar fashion as in *panel A*. Association with the mitochondrial membrane was ablated when more than 20 amino acids were deleted. *D*, import and fractionation of C-20 (*top panel*) and C-40^{35}S-labeled 3βHSD2 (*bottom panel*) after import into the isolated mitochondria is shown. After incubation with isolated mitochondria, the imported (*P*) fraction was separated from non-imported fraction (*S*) by washing and also by extraction with Na_2CO_3. The result shows C-20 and C-40 are processed in the same fashion of wild-type ^{35}S-labeled 3βHSD2. *E*, metabolic conversion of the deletion mutants cotransfected in COS-1 cells with F2. Data presented in *panel F* are the mean ± S.E. of three independent experiments. *U*, units; *Trilo*, trilostane.

extraction with sodium carbonate of NΔ2–5 3βHSD2 demonstrated that the deletion mutant (Fig. 7*B*, *bottom panel*) was imported with similar efficiency to wild-type 3βHSD2 (Fig. 7*B*, *top panel*). The fact that NΔ2–5 3βHSD2 was imported into the mitochondria but did not form a complex implies that import and translocase interaction are not the same. We next determined the minimum number of amino acids required for the generation of the 3βHSD2 complex by generating mutants with internal deletions of 15 amino acids (Fig. 7*B*). We found that the complex was restored to that of the wild type only when the mutant retained the first 15 amino acids (NΔ15–30). Coimmunoprecipitation of the NΔ15–30 3βHSD2 complex with the 3βHSD2 antibody did not show any interaction with the Tim50 or Tim23 translocases. To determine the biological activity of the different deletion mutants, we cotransfected COS-1 cells with 3βHSD2 and F2 (fusion of cytochrome P450scc-ferrodoxin-ferrodoxin reductase). As nonsteroidogenic COS-1 cells do not have any P450scc or ferrodoxin and ferrodoxin reductase, we provided these as a single fused protein, F2 (41, 42). Metabolic conversion of the transfected cells showed full activity with the wild-type 3βHSD2 but no activity with any of the deletion mutants, suggesting the N terminus association with the translocases is crucial for 3βHSD2 activity.

To investigate the role of the C terminus for interaction with Tim50, we deleted 3, 10, 20, 30, and 40 amino acids from the C terminus generating C-3, C-10, C-20, C-30, and C-40 3βHSD2 mutants. Import of the C-20 and C-40 mutants into isolated mitochondria, and isolation of the complex through native gradient PAGE after digitonin lysis showed that the complex containing C-20 3βHSD2 was similar in size to that of wild-type 3βHSD2. The complex was absent with the C-40 3βHSD2 mutant, suggesting that the C terminus plays a lesser role in the interaction with the associated proteins at the IMM. However, import of the C-20 and C-40 into mitochondria and extraction with sodium carbonate showed that both C-terminal deletion mutants were imported in a fashion similar to wild-type 3βHSD2 protein (Fig. 7*D*). Based on these results, it appears that N terminus and C terminus contribute differently to the interaction with IMM resident proteins.

DISCUSSION

For decades researchers have sought to identify the mechanisms of action of 3βHSD2 as well as its receptor. In this study we show that 3βHSD2 interacted with the IMM translocase, Tim50, from the C-terminal to the IMS side of the mitochondria and that this interaction helped to mediate 3βHSD2 metabolic activity. In the yeast model, Tim50 interacts with Tim23, facilitating the efficient transfer of proteins from the Tom40 complex to the Tim23 complex and facilitating the transport of proteins across the IMM by promoting the motor function of Hsp70 (11). Point mutations in the IMS domain of Tim50 reduce these activities, likely related to the degree of conformation change of the protein and the subsequent inability to interact with Tim23 (11, 43). The observed defects in motor functions are indirect consequence of growth defects (11), and this is due to the absence of steroids required for sexual development. Sugiyama *et al.* (44) found that *Drosophila* with mutations in the yeast Tim50 ortholog exhibit reduced growth and mitochondrial membrane potential. Similarly, in the human cell line 293T, Tim50 and Tim23 interact, and knockdown of Tim50 results in accelerated cytochrome *c* release and subsequent apoptosis. Developmental defects stemming from increased cell death are also seen in zebrafish with Tim50 knockdown (14). Given the interaction of Tim50 and Tim23 in the IMS, it was not surprisingly that 3βHSD2 also formed a transient association with Tim23. We also found an association with Tom22, a component of the Tom40 complex. Knockdown of Tim50 expression reduced the expression of 3βHSD2 by 80% as well as decreased 3βHSD2 activity. Even with the restoration of 3βHSD2 expression, 3βHSD2 remained inactive in Tim50 knockdown cells. Expression of an unrelated protein under identical conditions did not restore steroidogenic activity, sug-

gesting that the orientation of 3βHSD2 with Tim50 is essential. These results suggest that the presence of Tim50 is mandatory for 3βHSD2 docking at the IMS and that this promotes 3βHSD2 function. Patients with 3βHSD2 mutations had similar phenotypic expression, supporting a role for Tim50 in 3βHSD2 function. Introduction of wild-type Tim50 into the Tim50 knockdown cells restored 3βHSD2 activity; however, introduction of Tim50 mutants (11) that could not interact with Tim23 did not restore activity. Moreover, knockdown of either Tim23 or Tom22 reduced 3βHSD2 metabolic activity, supporting the notion that complex formation contributes to regulation of 3βHSD2 activity.

Tim50 also affected DHEA expression. P450c17 converts pregnenolone and progesterone to their 17 hydroxy forms and then converts those metabolites to DHEA and androstenedione. The 17,20-lyase activity of P450c17 is ~50 times more efficient for conversion of 17 OH pregnenolone to DHEA than for conversion of 17 OH progesterone to androstenedione; thus, P450c17 plays a crucial role in DHEA expression. Knockdown of translocases did not alter expression of P450c17, but knockdown of Tim50 reduced expression of DHEA (Fig. 4*E*). Thus, the reduced conversion of DHEA to androstenedione seen in Tim50 knockdown cells likely resulted from the reduced expression of 3βHSD2. Our results confirm, 3βHSD2 alone cannot catalyze the conversion of 17-hydroxy progesterone to DHEA. The absence of Tim23 or Tom22 did not inhibit DHEA expression, but minimally affected conversion, possibly due to the absence of 3βHSD2. In summary, DHEA expression requires the presence of Tim50 for the catalytic reaction. However, at this time we cannot predict how these proteins interact.

The Tom complex in the OMM and the Tim50 complex in the IMM are not permanently linked and can interact only in the presence of a translocating precursor protein (45–47). Therefore, a precursor pre-protein such as 3βHSD2, translocating through the Tom complex, must engage the Tim50 complex in the boundary inner membrane through the transient contact sites (48). The IMS domains of Tim23-Tim50 form a minimal binding interface required for the interaction of these two proteins. However, it is questionable whether Tim23 and Tim50 interact solely through their soluble domains given the lower K_d for the interaction (49). The transmembrane domain of Tim50 may stabilize flexible Tim23, resulting in a stable Tim23-Tim50 interaction (50). It is intriguing that the isolated IMS domains of Tim23 and Tim50 interact with each other despite the fact Tim23 is largely unfolded (49). The flexible 3βHSD2 was active as the protein retained similar binding capacity with its ligand trilostane (51). The flexibility of Tim23 seems essential, as it allows for docking Tim50 for stabilization and can thus connect transiently with Tom22. Indeed, proteolysis with trypsin confirms that 3βHSD2 has no protease-resistant domain. However, the interaction between the translocases and the 3βHSD2 is tightly regulated. This is possibly a mandatory condition for 3βHSD2 to adopt a conformation needed for interaction in a proper orientation with the translocases.

Mitochondrial-targeted protein import generally starts at the N terminus. After import, the N-terminal sequence, which contributes to sorting the protein to a specific location, may be cleaved. In this study 3βHSD2 is imported starting from the N terminus, but its N-terminal sequence is not cleaved, which also occurs for the IMM resident small Tim proteins (3). Deletion of three amino acids (NΔ2–5 3βHSD2) from the N terminus did not ablate the import but did inhibit its association with the mitochondrial translocases. To associate with the IMM resident proteins, 3βHSD2 required its first 15 amino acids (Δ15–30 3βHSD2) at the N terminus. However, this complex was unable to metabolize pregnenolone to progesterone. This might be the sole reason that patients with a change in the N-terminal amino acids of 3βHSD2 develop congenital adrenal hyperplasia (17). We believe that deletion of the small section of the 3βHSD2, especially from the N terminus, ablated activity due to the absence of interaction with the Tim50. Alternatively, the orientation of 3βHSD2 with Tim50 and Tom22 may be inhibited. The C terminus deletion of 10 amino acids had no major effect. Mutations of more than 30 (C-30 3βHSD2) amino acids only show severe phenotypic expression of sexual differentiation (21). The possibility exists that the C-terminal hydrophobic amino acids of 3βHSD2 remain within the proteins core (52) and do not participate in the interaction with the mitochondrial translocases. In summary, 3βHSD2 associates with the inner membrane translocases in a fashion that requires tight regulation, and any change in the expression of the inner mitochondrial translocase, Tim50, ablates steroidogenesis.

Acknowledgments—We are thankful to Drs. Toshio Endo for Tim50 and Walter Miller for the P450c17 antibody. Funding for equipment in the Mass Spectrometry Facility at the University of Alberta was supported by the Canada Foundation for Innovation and Alberta Science and Research Investment Program.

REFERENCES

1. Herrmann, J. M., and Neupert, W. (2000) *Curr. Opin. Microbiol.* **3,** 210–214
2. Schnell, D. J., and Hebert, D. N. (2003) *Cell* **112,** 491–505
3. Koehler, C. M. (2004) *Annu. Rev. Cell Dev. Biol.* **20,** 309–335
4. Neupert, W. (1997) *Annu. Rev. Biochem.* **66,** 863–917
5. Rehling, P., Brandner, K., and Pfanner, N. (2004) *Nat. Rev. Mol. Cell Biol.* **5,** 519–530
6. Neupert, W., and Herrmann, J. M. (2007) *Annu. Rev. Biochem.* **76,** 723–749
7. Kutik, S., Guiard, B., Meyer, H. E., Wiedemann, N., and Pfanner, N. (2007) *J. Cell Biol.* **179,** 585–591
8. Endo, T., Yamamoto, H., and Esaki, M. (2003) *J. Cell. Sci.* **116,** 3259–3267
9. Chacinska, A., Lind, M., Frazier, A. E., Dudek, J., Meisinger, C., Geissler, A., Sickmann, A., Meyer, H. E., Truscott, K. N., Guiard, B., Pfanner, N., and Rehling, P. (2005) *Cell* **120,** 817–829
10. de la Cruz, L., Bajaj, R., Becker, S., and Zweckstetter, M. (2010) *Protein Sci.* **19,** 2045–2054
11. Tamura, Y., Harada, Y., Shiota, T., Yamano, K., Watanabe, K., Yokota, M., Yamamoto, H., Sesaki, H., and Endo, T. (2009) *J. Cell Biol.* **184,** 129–141
12. Bolender, N., Sickmann, A., Wagner, R., Meisinger, C., and Pfanner, N. (2008) *EMBO Rep.* **9,** 42–49
13. Meinecke, M., Wagner, R., Kovermann, P., Guiard, B., Mick, D. U., Hutu, D. P., Voos, W., Truscott, K. N., Chacinska, A., Pfanner, N., and Rehling, P. (2006) *Science* **312,** 1523–1526
14. Guo, Y., Cheong, N., Zhang, Z., De Rose, R., Deng, Y., Farber, S. A., Fernandes-Alnemri, T., and Alnemri, E. S. (2004) *J. Biol. Chem.* **279,** 24813–24825
15. Yamamoto, H., Esaki, M., Kanamori, T., Tamura, Y., Nishikawa, S., and Endo, T. (2002) *Cell* **111,** 519–528

16. Mokranjac, D., Paschen, S. A., Kozany, C., Prokisch, H., Hoppins, S. C., Nargang, F. E., Neupert, W., and Hell, K. (2003) *EMBO J.* **22,** 816–825
17. Miller, W. L., and Auchus, R. J. (2011) *Endocr. Rev.* **32,** 81–151
18. Simard, J., Ricketts, M. L., Gingras, S., Soucy, P., Feltus, F. A., and Melner, M. H. (2005) *Endocr. Rev.* **26,** 525–582
19. Nair, K. S., Rizza, R. A., O'Brien, P., Dhatariya, K., Short, K. R., Nehra, A., Vittone, J. L., Klee, G. G., Basu, A., Basu, R., Cobelli, C., Toffolo, G., Dalla, Man, C., Tindall, D. J., Melton, L. J., 3rd, Smith, G. E., Khosla, S., and Jensen, M. D. (2006) *N. Engl. J. Med.* **355,** 1647–1659
20. Labrie, F., Luu-The, V., Labrie, C., and Simard, J. (2001) *Front. Neuroendocrinol.* **22,** 185–212
21. Welzel, M., Wüstemann, N., Simic-Schleicher, G., Dörr, H. G., Schulze, E., Shaikh, G., Clayton, P., Grötzinger, J., Holterhus, P. M., and Riepe, F. G. (2008) *J. Clin. Endocrinol. Metab.* **93,** 1418–1425
22. Brière, N., Martel, D., Cloutier, M., and LeHoux, J. G. (1997) *J. Histochem. Cytochem.* **45,** 1409–1416
23. Praporski, S., Ng, S. M., Nguyen, A. D., Corbin, C. J., Mechler, A., Zheng, J., Conley, A. J., and Martin, L. L. (2009) *J. Biol. Chem.* **284,** 33224–33232
24. Nakajin, S., and Hall, P. F. (1981) *J. Biol. Chem.* **256,** 3871–3876
25. Bose, M., Adams, B. P., Whittal, R. M., and Bose, H. S. (2008) *Electrophoresis* **29,** 753–760
26. Bose, M., Debnath, D., Chen, Y., and Bose, H. S. (2007) *J. Mol. Endocrinol.* **39,** 67–79
27. Schwartz, M. P., and Matouschek, A. (1999) *Proc. Natl. Acad. Sci. U.S.A.* **96,** 13086–13090
28. Komarov, A. G., Deng, D., Craigen, W. J., and Colombini, M. (2005) *Biophys. J.* **89,** 3950–3959
29. Rosenfeld, J., Capdevielle, J., Guillemot, J. C., and Ferrara, P. (1992) *Anal. Biochem.* **203,** 173–179
30. Thomas, J. L., Myers, R. P., and Strickler, R. C. (1989) J. *Steroid Biochem.* **33,** 209–217
31. Thomas, J. L., Mack, V. L., Sun, J., Terrell, J. R., and Bucholtz, K. M. (2010) *J. Steroid Biochem. Mol. Biol.* **120,** 192–199
32. Schatz, G., and Dobberstein, B. (1996) *Science* **271,** 1519–1526
33. Bose, H. S., Sugawara, T., Strauss, J. F., 3rd, and Miller, W. L. (1996) *N. Engl. J. Med.* **335,** 1870–1878
34. Bellot, G., Cartron, P. F., Er, E., Oliver, L., Juin, P., Armstrong, L. C., Bornstein, P., Mihara, K., Manon, S., and Vallette, F. M. (2007) *Cell Death Differ.* **14,** 785–794
35. van Wilpe, S., Ryan, M. T., Hill, K., Maarse, A. C., Meisinger, C., Brix, J., Dekker, P. J., Moczko, M., Wagner, R., Meijer, M., Guiard, B., Hönlinger, A., and Pfanner, N. (1999) *Nature* **401,** 485–489
36. Court, D. A., Nargang, F. E., Steiner, H., Hodges, R. S., Neupert, W., and Lill, R. (1996) *Mol. Cell. Biol.* **16,** 4035–4042
37. Moczko, M., Bömer, U., Kübrich, M., Zufall, N., Hönlinger, A., and Pfanner, N. (1997) *Mol. Cell. Biol.* **17,** 6574–6584
38. Woody, R. W., and Dunker, A. K. (1996) in *Circular Dichroism and Conformational Analysis of Biomolecules*, pp. 109–158 (Fasman, G. D., ed) Plenum Press, New York
39. Johnson, W. C., Jr. (1988) *Annu. Rev. Biophys Biophys Chem* **17,** 145–166
40. Tinker, D. A., Krebs, E. A., Feltham, I. C., Attah-Poku, S. K., and Ananthanarayanan, V. S. (1988) *J. Biol. Chem.* **263,** 5024–5026
41. Black, S. M., Szklarz, G. D., Harikrishna, J. A., Lin, D., Wolf, C. R., and Miller, W. L. (1993) *Endocrinology* **132,** 539–545
42. Harikrishna, J. A., Black, S. M., Szklarz, G. D., and Miller, W. L. (1993) *DNA Cell Biol.* **12,** 371–379
43. Bose, H. S., Baldwin, M. A., and Miller, W. L. (1998) *Biochemistry* **37,** 9768–9775
44. Sugiyama, S., Moritoh, S., Furukawa, Y., Mizuno, T., Lim, Y. M., Tsuda, L., and Nishida, Y. (2007) *Genetics* **176,** 927–936
45. Berthold, J., Bauer, M. F., Schneider, H. C., Klaus, C., Dietmeier, K., Neupert, W., and Brunner, M. (1995) *Cell* **81,** 1085–1093
46. Horst, M., Hilfiker-Rothenfluh, S., Oppliger, W., and Schatz, G. (1995) *EMBO J.* **14,** 2293–2297
47. Dekker, P. J., Martin, F., Maarse, A. C., Bömer, U., Müller, H., Guiard, B., Meijer, M., Rassow, J., and Pfanner, N. (1997) *EMBO J.* **16,** 5408–5419
48. Pfanner, N., Rassow, J., van der Klei, I. J., and Neupert, W. (1992) *Cell* **68,** 999–1002
49. Gevorkyan-Airapetov, L., Zohary, K., Popov-Celeketic, D., Mapa, K., Hell, K., Neupert, W., Azem, A., and Mokranjac, D. (2009) *J. Biol. Chem.* **284,** 4865–4872
50. Pfanner, N. (2000) *Curr. Biol.* **10,** R412–R415
51. Thomas, J. L., Bucholtz, K. M., Sun, J., Mack, V. L., and Kacsoh, B. (2009) *Mol. Cell. Endocrinol.* **301,** 174–182
52. Thomas, J. L., Duax, W. L., Addlagatta, A, Brandt, S., Fuller, R. R., and Norris, W. (2003) *J. Biol. Chem.* **278,** 35483–35490